Int. J. Heat Mass Transfer. Vol. 33, No. 8, pp. 1711–1720, 1990
Printed in Great Britain

0017–9310/90 $3.00 + 0.00

Heat transfer in developing magnetohydrodynamic Poiseuille flow and variable transport properties

ALIREZA SETAYESH†
Mechanical Engineering Department, Tuskegee University, Tuskegee, AL 36088, U.S.A.

and

VIRESHWAR SAHAI
Mechanical Engineering Department, Tennessee Technological University, Cookeville, TN 38505, U.S.A.

(*Received* 15 *March* 1989 *and in final form* 20 *October* 1989)

Abstract—A study is made of the effect of temperature-dependent transport properties on the developing magnetohydrodynamic flow and heat transfer in a parallel-plate channel whose walls are held at constant and equal temperatures. The flow is assumed to be steady, laminar, and incompressible. Representative numerical results are presented to show that the variation of properties may, under certain circumstances, have a significant influence on the development of both velocity and temperature profiles.

INTRODUCTION

THE STUDY of magnetohydrodynamic (MHD) flow and heat transfer has important applications in such devices as MHD generators. The flow in an MHD generator channel is seldom fully developed over its entire length, and large heat fluxes occur at the entrance regions of these devices. In addition, because the generator usually operates at high temperatures, the flow transport properties are strong functions of temperature. This temperature dependence is likely to affect the flow and heat transfer characteristics of the generator channel significantly. The objective of the present investigation is to study the effect of temperature-dependent transport properties on the velocity and temperature profiles in the entrance region of a parallel-plate channel whose walls are held at constant and equal temperatures. This developing MHD Poiseuille flow is assumed to be incompressible, steady, and laminar.

In a pioneering paper, Rosa [1] has discussed the effect of variable transport properties in MHD channel flow from both the experimental and theoretical points of view. The studies by Thompson and Bopp [2], Heywood [3], Filippov [4], and Setayeshpour [5] of fully developed MHD channel flows, which include both the Poiseuille and Couette flow configurations, have shown that deviations from constant transport properties have a significant effect on the heat transfer characteristics of the channel.

The problem of developing MHD flow and heat transfer has been the subject of many investigations. Most of these studies, however, assume constant transport properties for the fluid. The constant-property developing MHD flow has been investigated both by approximate integral analyses (refs. [6–9], for example) and by finite difference methods such as those used by Hwang [10] and Shohet [11]. In the non-MHD case, the effect of variable viscosity on developing flow and heat transfer has been extensively investigated; the work of McKillop *et al.* [12] is typical of such studies.

General power-law relationships have been used in this study to describe the transport properties of the fluid. The properties of many fluids of interest can be accurately represented by such relationships. However, no specific fluid has been kept in mind in the present parametric study. Instead, the emphasis is on determining the effect of variation of the exponents in the power-law relationships on the flow and heat transfer characteristics of the channel. The study of developing magnetohydrodynamic flow, which takes the variation of properties with temperature into account, has been the subject of only a few recent investigations. For example, Lohrasbi [13] has considered the variation of transport properties with temperature in a one-dimensional, two-phase MHD flow. Mittal *et al.* [14] have studied the developing flow and heat transfer in an electrode wall channel of two plasmas with variable transport properties. It is not possible, however, to compare their results with the present study because of the differences in boundary conditions. Setayeshpour and Sahai [15] have discussed the effect of temperature-dependent transport properties in the entrance region of an MHD channel flow. They used a generalized type of temperature

† Present address: Radex, Inc., Three Preston Court, Bedford, MA 01730, U.S.A.

NOMENCLATURE

B_0	applied magnetic field
C_p	specific heat at constant pressure
d	width of channel
D_e	equivalent diameter, $2L$
Ek	Eckert number
E_z	electric field
Gz	Graetz number
h	heat transfer coefficient
I_T	total current across the channel
J_z	current density
k	thermal conductivity
L	height of the channel
M	Hartmann number
M_{eff}	effective Hartmann number
N	number of steps in the mesh network
Nu	Nusselt number
p	pressure
Pr	Prandtl number
Q	total heat flux from entry to an arbitrary location in the x-direction of the channel
R_E	electric field parameter
T	temperature of the fluid
T_b	bulk temperature
U	average velocity
u, v	velocity components.

Greek symbols

α	viscosity exponent
β	electrical conductivity exponent
γ	thermal conductivity exponent
θ	temperature ratio appearing in power-law relationships
μ	variable viscosity of the fluid
ρ	density of the fluid
σ	variable electrical conductivity of the fluid.

Subscripts

e	entrance condition
m	average condition
w	wall (plate) condition.

boundary condition, in which the wall heat flux is assumed to be a linear function of local wall temperature.

It should also be noted that several general purpose codes have been developed to analytically model a wide variety of MHD generation devices in a realistic manner. Demetriades *et al.* [16] present an excellent survey of the capabilities of these codes, some of which include variable property effects. The purpose of the present study, however, is not to model a specific situation or a device but to investigate the effect of variation of properties in an idealized, simple situation. Since, as far as the authors are aware, no experimental results are available for the variable property case for the problem considered here, the results presented here do not pertain to a specific fluid.

Finally, it is worth pointing out that the present study has important applications in areas other than MHD power generation. Entry length effects are also important, for example in liquid metal fusion blankets [17].

GOVERNING EQUATIONS

The geometry of the MHD parallel-plate channel is shown in Fig. 1. The height of the channel is L and is taken to be much smaller than the width of the channel d. The velocity and temperature profiles develop toward the direction of increasing x, and the external magnetic fields are applied in the positive y-direction. The two parallel plates are considered to be electrically insulated. Two electrically conducting plates are assumed to be placed in planes parallel to the x–y plane at distances of $1/2d$ and $-1/2d$ from the origin. These plates enclose the outside of the channel if d is sufficiently large, they will not affect the velocity and temperature profile development in the middle portion of the channel, as was illustrated by Hughes and Young [18].

A number of assumptions have been made in order to simplify the problem and to be consistent with the physical geometry of the problem. The flow is considered to be laminar and steady, and there are no applied (external) magnetic fields other than the one in the y-direction. None of the quantities are allowed to vary in the z-direction. The induced magnetic field is considered to be small, and the Hall and ion-slip effects are assumed to be negligible. The velocity and temperature gradients of the x component of momentum and energy equations respectively taken in the y-

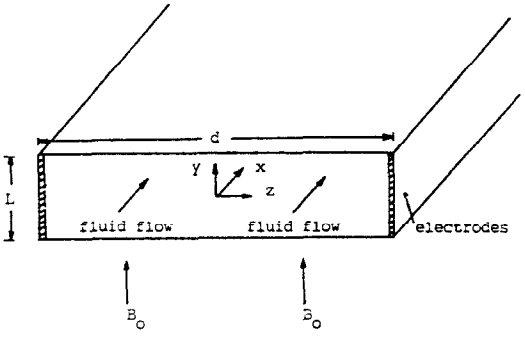

FIG. 1. Geometry of the parallel-plate channel.

direction dominate all other velocity and temperature gradients. Any externally imposed electrical fields are assumed to act in the z-direction only.

From the preceding assumptions, it is possible to make boundary layer-type approximations for analyzing developing flow and, therefore, the governing equations of MHD channel flow under consideration can be stated as follows:

$$\frac{\partial u}{\partial x}+\frac{\partial v}{\partial y}=0 \tag{1}$$

$$\rho\left(u\frac{\partial u}{\partial x}+v\frac{\partial v}{\partial y}\right)=-\frac{\mathrm{d}p}{\mathrm{d}x}+\frac{\partial}{\partial y}\left(\mu\frac{\partial u}{\partial y}\right)-\sigma B_0(E_z+uB_0) \tag{2}$$

$$\rho C_p\left(u\frac{\partial T}{\partial x}+v\frac{\partial T}{\partial y}\right)=\frac{\partial}{\partial y}\left(k\frac{\partial T}{\partial y}\right)+\mu\left(\frac{\partial u}{\partial y}\right)^2+\sigma(E_z+uB_0)^2. \tag{3}$$

Here u and v are the velocity components, p the pressure, E_z the electric field and B_0 the applied magnetic field. The density ρ and specific heat C_p are assumed to be constant. The equations are written in a form which permits the possible variation of the electrical conductivity σ, viscosity μ and thermal conductivity k as functions of temperature. In addition to the standard boundary layer assumptions, the above equations implicitly assume that the induced magnetic field is small and Hall and ion-slip effects are negligible.

In the temperature range in which an MHD generator operates, the viscosity and electrical and thermal conductivities may be strong functions of temperature. In the present study, the following power-law relationships are assumed for viscosity and electrical and thermal conductivities:

$$\mu=\mu_w\left(\frac{T}{T_w}\right)^{\alpha} \tag{4}$$

$$\sigma=\sigma_w\left(\frac{T}{T_w}\right)^{\beta} \tag{5}$$

$$k=k_w\left(\frac{T}{T_w}\right)^{\gamma} \tag{6}$$

where T_w is the wall temperature, and the quantities μ_w, σ_w, and k_w represent, respectively, the value of the viscosity, electrical conductivity, and thermal conductivity at the wall. It should be noted that the above power-law relationships have been suggested by numerous authors, for example refs. [1–4, 19] for MHD flows.

The governing equations can be non-dimensionalized using the following set of dimensionless variables and parameters based upon the characteristic width of the channel L, mean velocity U and wall temperature T_w:

$$x^*=\frac{\mu_w x}{L^2\rho U},\quad y^*=\frac{y}{L},\quad u^*=\frac{u}{U}$$

$$v^*=\frac{L\rho v}{\mu_w},\quad \mu^*=\frac{\mu}{\mu_w},\quad \sigma^*=\frac{\sigma}{\sigma_w},\quad k^*=\frac{k}{k_w}$$

$$p^*=\frac{p-p_0}{\rho U^2},\quad T^*=\frac{T-T_w}{T_e-T_w},\quad M=B_0L\left(\frac{\sigma_w}{\mu_w}\right)^{1/2}$$

$$Pr=\frac{\mu_w C_p}{k},\quad R_E=\frac{E_z}{UB_0},\quad Ek=\frac{U^2}{C_p(T_e-T_w)}.$$

Here, M, Pr, and Ek are respectively the Hartmann, Prandtl, and Eckert numbers, and R_E the electric loading parameter. T_w is the temperature of the wall. Then equations (1)–(3), in their non-dimensional forms, can now be written as

$$\frac{\partial u}{\partial x}+\frac{\partial v}{\partial y}=0 \tag{7}$$

$$u\frac{\partial u}{\partial x}+v\frac{\partial v}{\partial y}=-\frac{\mathrm{d}p}{\mathrm{d}x}+\frac{\partial}{\partial y}\left(\mu\frac{\partial u}{\partial y}\right)-\sigma M^2(R_E+u) \tag{8}$$

$$u\frac{\partial T}{\partial x}+v\frac{\partial T}{\partial y}=\frac{1}{Pr}\frac{\partial}{\partial y}\left(k\frac{\partial T}{\partial y}\right)+Ek\mu\left(\frac{\partial u}{\partial y}\right)^2+Ek\sigma M^2(R_E+u)^2 \tag{9}$$

where, for convenience, the asterisks have been dropped with the understanding that all quantities are now non-dimensional. The power-law relationships of equations (4)–(6) acquire the following non-dimensional form:

$$\mu=(1+\theta T)^{\alpha} \tag{10}$$

$$\sigma=(1+\theta T)^{\beta}\quad \beta\geq 0 \tag{11}$$

$$k=(1+\theta T)^{\gamma}\quad \gamma\geq 0 \tag{12}$$

where

$$\theta=\frac{T_e}{T_w}-1.$$

The above equations must be solved subject to appropriate initial and boundary conditions. It will be assumed here that at the entrance of the channel both velocity and temperature are uniform. These initial conditions can be stated in the following non-dimensional form:

$$\text{at}\quad x=0,\quad \text{for}\quad -\tfrac{1}{2}<y<\tfrac{1}{2},\quad u=1,\quad v=0,\quad T=1,\quad \text{and}\quad p=0. \tag{13}$$

The no-slip boundary conditions apply at channel walls for velocity. The temperature at the walls is taken to be constant and equal to T_w. The non-dimensional forms of these conditions can be written as follows:

$$\text{for}\quad x\geq 0,\quad \text{at}\quad y=\pm\tfrac{1}{2},\quad u=0,\quad v=0,\quad T=0. \tag{14}$$

The Hartmann number M is based upon viscosity and electrical conductivity values at the wall temperature. When these properties are taken to be temperature-dependent, the effective Hartmann number can often be very different from its reference value. Thus, knowing the actual Hartmann number M in the channel can be helpful in explaining some of the results in this work.

The actual Hartmann number at a given location in the channel can be defined as follows:

$$M_{\text{eff}} = B_0 L\left(\frac{\sigma}{\mu}\right)^{1/2}. \tag{15}$$

Here the viscosity μ and electrical conductivity σ are the dimensional variables. Thus, equation (15) in non-dimensional variables can be written as

$$M_{\text{eff}} = M\left(\frac{\sigma}{\mu}\right)^{1/2} \tag{16}$$

where parameters σ and μ are given by equations (5) and (4), respectively.

The total current per unit of channel length is given by

$$I_T = \int_{-1/2L}^{1/2L} J_z \, dy. \tag{17}$$

The current density J_z in the above equation is given by Ohm's law as follows:

$$J_z = \sigma(E_z + uB_0). \tag{18}$$

The total current in dimensionless form can now be written as

$$I_T = \int_{-1/2}^{1/2} \sigma(R_E + u)\, dy. \tag{19}$$

Note that for the open circuit case ($I_T = 0$), the value of R_E becomes a function of variable electrical conductivity σ and can be determined from the above equation as follows:

$$R_E = -\frac{\int_{-1/2}^{1/2} \sigma u \, dy}{\int_{-1/2}^{1/2} \sigma \, dy}. \tag{20}$$

There are some additional parameters which have been used in this work which need to be defined; for example, the bulk temperature is calculated by

$$T_b = \frac{\int_{-1/2L}^{1/2L} uT \, dy}{\int_{-1/2L}^{1/2L} u \, dy} \tag{21}$$

which, in non-dimensional form, becomes

$$T_b = \int_{-1/2}^{1/2} uT \, dy \tag{22}$$

where

$$\int_{-1/2}^{1/2} u \, dy = 1. \tag{23}$$

The average Nusselt number, in its usual form, is given by

$$Nu_m = \frac{h_m D_e}{k_m}. \tag{24}$$

For a rectangular channel with height L, the equivalent diameter D_e is equal to $2L$. The average heat transfer coefficient h_m for a length x of channel (and unit width) in which there is heat transfer at both walls is given by

$$h_m = \frac{Q}{A\Delta T} = \frac{Q}{(2x)(\Delta T)} \tag{25}$$

where Q is the total heat flux from the entry to x and is defined as

$$Q = 2\int_0^x -k\left(\frac{\partial T}{\partial y}\right)_{\text{wall}} dx. \tag{26}$$

The temperature difference, ΔT, is defined by

$$\Delta T = \frac{(T_e - T_w) - (T_{b,x} - T_w)}{\ln \dfrac{T_e - T_w}{T_{b,x} - T_w}}. \tag{27}$$

Since the thermal conductivity is assumed to be a function of temperature, a mean thermal conductivity k_m has been defined as follows:

$$k_m = \frac{k_e + k_{m,x}}{2}. \tag{28}$$

Here k_e is the thermal conductivity at entrance temperature and $k_{m,x}$ is the mean thermal conductivity at a given location of x, which in non-dimensional form can be defined as

$$k_{m,x} = (1 + \theta T_{b,x})^{\gamma}. \tag{29}$$

Therefore, the mean Nusselt number in non-dimensional quantities can now be stated as

$$Nu_m = \frac{\dfrac{4}{x\Delta T}\displaystyle\int_0^x -k\left(\frac{\partial T}{\partial y}\right)_{\text{wall}} dx}{(1+\theta)^{\gamma} + (1 + \theta T_{b,x})^{\gamma}} \tag{30}$$

where ΔT is given by the following equation:

$$\Delta T = \frac{T_{b,x} - 1}{\ln T_{b,x}}. \tag{31}$$

The average Nusselt number will be plotted versus the Graetz number which is defined as

$$Gz = \frac{R_L Pr}{(x/2L)} \tag{32}$$

where R_L is the equivalent Reynolds number, which is defined as

$$R_L = \frac{2\rho UL}{\mu_w}. \tag{33}$$

In terms of the dimensionless quantities defined earlier, Gz can be expressed as follows:

$$Gz = \frac{4}{x} Pr. \tag{34}$$

METHOD OF SOLUTION

The coupled governing equations of continuity, momentum, and energy (equations (7)–(9)) for developing flow and heat transfer are solved subject to the initial conditions (13) and boundary conditions (14). Additional coupling and non-linearities are introduced by the assumption of variable properties. The coupled, non-linear governing equations are solved in the present investigation by a finite difference marching procedure developed by Patankar and Spalding [20].

To implement this implicit scheme, the x and y derivatives are approximated by forward and central differences, respectively. After the non-linear terms have been suitably linearized in the finite difference form, this procedure leads to a set of tridiagonal equations which can be solved by an efficient successive-substitution scheme. It should be noted that the procedure used here is the one for confined flows. The pressure is not directly specified for confined flow and must be determined at every step as a part of the marching procedure.

The iteration process needed to handle the temperature-dependent properties proceeds as follows. As the solution is marched in the axial direction (x axis), the current values of transport properties are calculated using the computed temperature distribution from the previous x station. At the same time, the inertia terms of the momentum and energy equations are linearized by substituting the previous values of velocity components u and v in those terms for the current x station. The current values of the velocity and temperature distributions are then calculated by solving the momentum and energy equations. The values of the transport properties are calculated again using these new values of velocity u and velocity v in the inertia terms of the momentum and energy equations. Iteration is then performed until the changes in u and v velocities are below a specified tolerance.

A point should be made about the velocity and temperature singularities at the channel's entrance. The initial condition for velocity requires that $u = 1$ at the entrance; however, at the edges of the two walls u may have a value different from unity because of the no-slip boundary condition. Nevertheless, the condition in equation (23) must be satisfied at every section along the channel, including the one at the entrance. The discrepancy caused by the singularities cannot be disregarded because it introduces irregularities in the computed velocity distribution. A simple and effective way to overcome the undesirable effects of the singularities is to distribute them over all the grid points. Therefore, the following relationship can be formulated:

$$\text{at} \quad x = 0 \quad \text{for} \quad -\tfrac{1}{2} < y < \tfrac{1}{2}, \quad u = 1 + \frac{1}{N-1} \tag{35}$$

where N represents the number of steps in the numerical solution. Any inaccuracies introduced by this assumption tend to diminish as N increases.

RESULTS

Employing the method described above, the governing equations of the problem can be solved for various values of the parameters θ, M, Pr, Ek, α, β, γ, and R_E. It is obviously not possible to consider here all possible combinations of these parameters. Therefore a major portion of the following discussion will concentrate on the effect of variation of α, β, and γ, the exponents in the power-law dependence of the transport properties on temperature. It must be recognized, however, that the other parameters can have a strong influence on the temperature distribution and the coupling between the momentum and energy equations. The values of θ, M, Ek, and R_E may therefore have an important bearing on how the developmental flow and heat transfer are affected by the variation of α, β, and γ [21].

The objective of the present paper is to discuss the effect of variable transport properties qualitatively, and the results presented here do not apply to any specific fluid or situation. Generally speaking, however, the viscosity of gases increases with temperature; therefore, the exponent α has a positive value. On the other hand, the viscosity of liquid decreases with temperature resulting in a negative value of α. It should be noted that the values of Prandtl number used in this work are 0.75 and 1.0. These values usually represent the Prandtl number of gases. However, since this work is not applicable to any specific fluid, for the purpose of comparison the same values of the Prandtl number have also been used for liquids.

In the case of constant properties, the present computations are compared to those of Shohet [11], Flegal [22], Hwang [10], Chen and Chen [23], Schlichting [24], Bodoia and Osterle [25], Roidt and Cess [26], and Manohar [27]. Table 1 shows a comparison of entrance or developmental lengths for velocity, using the criterion of 99% fully developed profiles, for different values of Hartmann number M. The values of entrance length at $M = 50$ and 100 are included to demonstrate the versatility of the present method. The corresponding results are not available in the

Table 1. Comparison of entrance lengths for velocity

	$M = 0$	$M = 8$	$M = 20$	$M = 50$	$M = 100$
Chen and Chen [23]	—	0.01732	0.00205	—	—
Hwang [10]	0.0422	0.0188	0.00304	—	—
Schlichting [24]	0.0400	—	—	—	—
Bodoia and Osterle [25]	0.044	—	—	—	—
Roidt and Cess [26]	0.0454	0.01670	—	—	—
Manohar [27]	0.0439	0.02	0.00307	—	—
Present work	0.04465	0.02080	0.00300	0.00021	0.00003

literature. Figures 2 and 3 compare the work of Shohet [11] with the present investigation with respect to the velocity distribution in the channel for two cases (Hartmann number $M = 4$ and 18, respectively) of developing MHD flow. The two results are in good agreement and the figures clearly show the characteristic effect of increasing Hartmann number on velocity. As M is increased, the velocity in the center portion of the channel ($y = 0$ represents the centerline) decreases. This is due to the overall retarding effect of the electromagnetic body force $\mathbf{J} \times \mathbf{B}$ (Lorentz force). The Hartmann number M represents the ratio of the Lorentz force to the viscous force in the fluid. The velocity near the walls increases somewhat in order to keep the mass flow rate constant.

Figure 4 presents the comparison of the velocity profile of an experimental investigation done by Flegal [22] with the computational data of the present work. The experiment was performed in an MHD channel with ratio of $d/L = 4$, and the experimental fluid was a potassium chloride solution. The test was conducted at room temperature; therefore, the variation of transport properties can be assumed to be negligible. Figure 4 shows the velocity distributions at two locations for an MHD flow with a Hartmann number of 5.8. As can be observed from the above figure, the experimental results of Flegal [22] and the computational results of the present investigation are very close.

Figure 5 shows the bulk temperature development along the channel for $M = 20$. In this figure the results of the present investigation are compared to the numerical results of Hwang [10]. The curves are plotted for two values of electric field parameter, $R_E = 0$ (short circuit) and -0.5. Similarly, the variation of average Nusselt number in the axial direction is compared to the work of Hwang in Fig. 6. It should be noted that in this graph the Nusselt numbers are based on log mean temperatures as described in equations (30) and (31). The two cases of $R_E = 0$ (short circuit) and $Ek = 1.0$, and $R_E = -1.0$ (open circuit) and

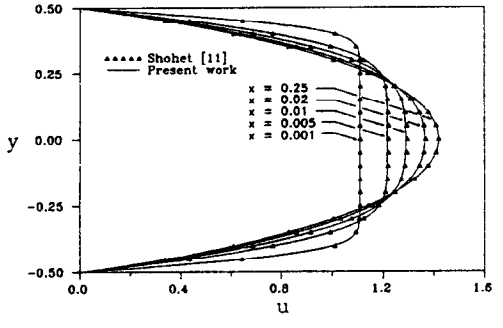

FIG. 2. Development of velocity profile along the channel for $M = 4.0$.

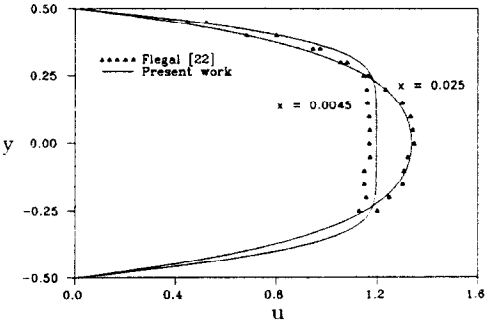

FIG. 4. Development of velocity profile along the channel for $M = 5.8$.

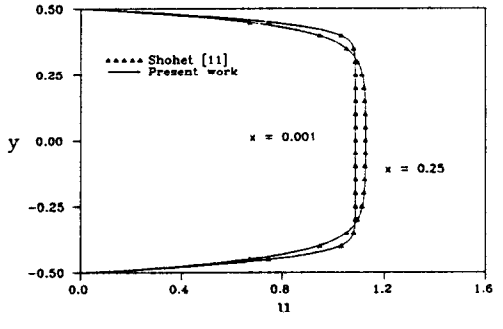

FIG. 3. Development of velocity profile along the channel for $M = 18.0$.

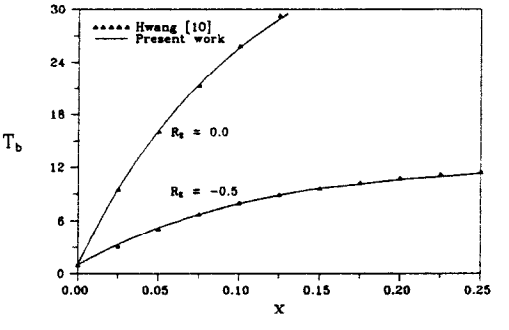

FIG. 5. Development of bulk temperature along the channel for $M = 20.0$, $Pr = 1.0$, and $Ek = 1.0$.

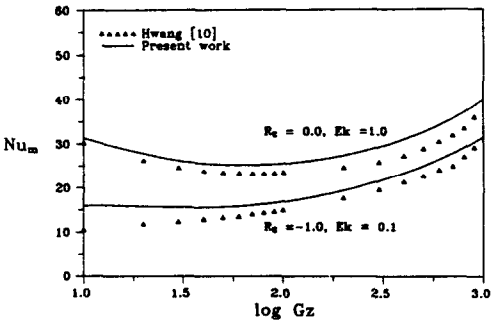

FIG. 6. Variation of average Nusselt number vs log of Graetz number for $M = 20.0$ and $Pr = 1.0$.

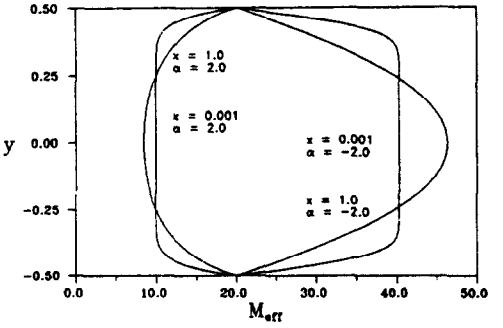

FIG. 9. Variation of effective Hartmann number across the channel for $M = 20.0$, $R_E = -0.5$, $Pr = 0.75$, $Ek = 0.1$, $\theta = 1.0$, $\beta = 0.0$, and $\gamma = 0.0$.

$Ek = 0.1$ are considered in the graph. The results presented above show that the numerical method used to solve the problem gives accurate results for developing MHD flow with constant transport properties. Some results for developing MHD flow with temperature-dependent transport properties are presented next.

Figures 7 and 8 show the development of axial velocity profiles in the channel for Hartmann number $M = 20$; the viscosity is assumed to vary with temperature, and the other properties are held constant to isolate the effect of viscosity variation. The results for the case in which all properties are constant are included in both figures for comparison purposes. In Fig. 7, for $\alpha = -2.0$ (negative exponent characterizes a liquid), the velocity is less in the central portion of the channel and larger near the plates ($y = 0.4$) when compared to the constant property case. In Fig. 8, in which $\alpha = 2.0$, representing gas flow, the effect on velocity is opposite. These effects are contrary to what would be expected in ordinary flow (non-MHD flow). This phenomenon can be understood by observing the relative effect of the electromagnetic force (Lorentz force) and the viscous force on the velocity distribution in a given situation. Since the Hartmann number represents the ratio of these two forces, it is interesting to investigate the variation of the effective Hartmann number along the channel. Figure 9 illustrates the variation of the actual Hartmann number for two cases, $\alpha = 2.0$ and -2.0, with conditions corresponding to those in Figs. 7 and 8. It is seen that for negative or positive α the effective Hartmann number varies considerably across the channel. These changes occur because, as temperature increases, the viscous force increases or decreases depending upon the sign of α. For negative α, the large increase in the effective Hartmann number significantly retards the flow in the central portion of the channel. In the case of positive α, on the other hand, the reduced values of the actual Hartmann number result in a less effective Lorentz force, and flow is not decelerated in the middle portion of the channel.

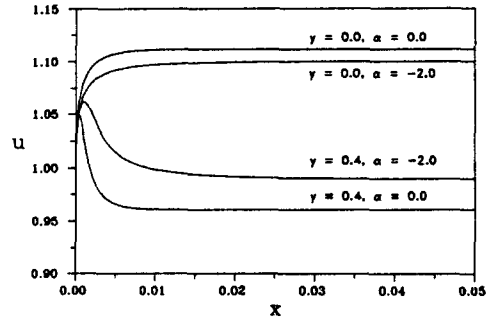

FIG. 7. Development of axial velocity for $M = 20.0$, $R_E = -0.5$, $Pr = 0.75$, $Ek = 0.1$, $\theta = 1.0$, $\beta = 0.0$, and $\gamma = 0.0$.

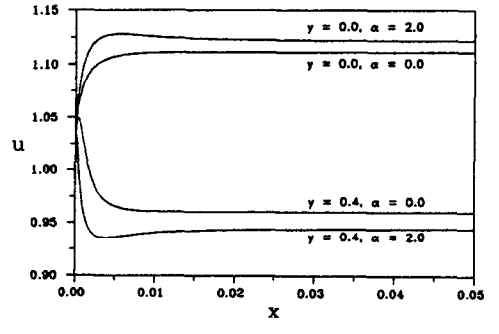

FIG. 8. Development of axial velocity for $M = 20.0$, $R_E = -0.5$, $Pr = 0.75$, $Ek = 0.1$, $\theta = 1.0$, $\beta = 0.0$, and $\gamma = 0.0$.

Figure 10 shows the effect of variable electrical conductivity on the velocity distribution across the channel for different locations in the axial direction. The exponents α and γ are taken to be zero. As Fig. 10

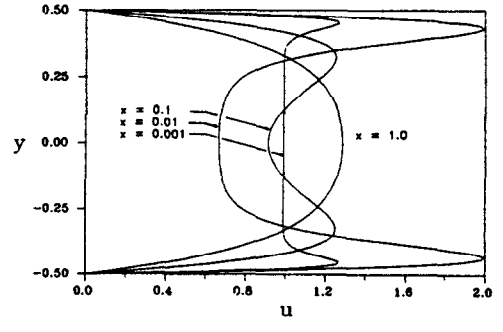

FIG. 10. Development of velocity profile along the channel for $M = 8.0$, $R_E = 0.0$, $Pr = 0.75$, $Ek = 0.0$, $\theta = 1.0$, $\alpha = 0.0$, $\beta = 5.0$, and $\gamma = 0.0$.

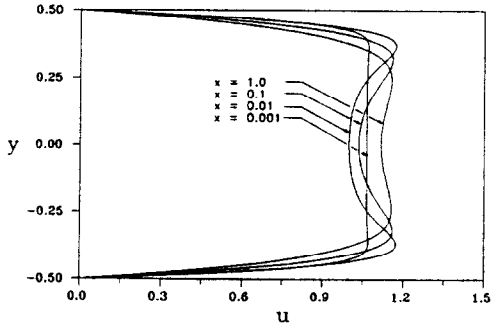

FIG. 11. Development of velocity profile along the channel for $M = 8.0$, $R_E = -0.8$, $Pr = 0.75$, $Ek = 0.2$, $\theta = 0.75$, $\alpha = 0.5$, $\beta = 5.0$, and $\gamma = 1.0$.

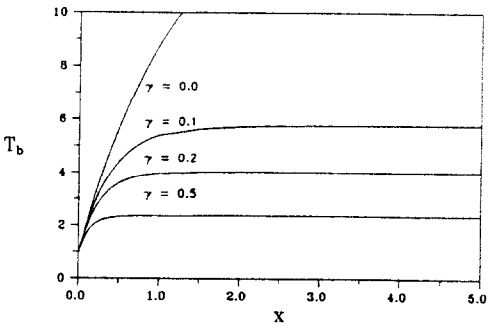

FIG. 12. Development of bulk temperature along the channel for $M = 20.0$, $R_E = -0.5$, $Pr = 1.0$, $Ek = 0.1$, $\theta = 1.0$, $\alpha = 2.0$, and $\beta = 1.0$.

shows, the flow becomes retarded in the central portion and accelerated near the walls. This produces an overshoot velocity in the neighborhood of the walls and results in an M-shaped velocity profile. The cause of this pattern may be determined by examining the temperature distribution. Although the results are not presented here, the temperature is much higher in the central region as compared to that near the walls. This causes a large increase in the electrical conductivity σ in the core region of the channel. As a result, the Lorentz force, which is a retarding force, becomes stronger in the central portion than near the walls. It is interesting to see what happens to the overshoot velocity pattern as the flow develops along the channel, the velocity profile gradually loses its M-shape and assumes a characteristic parabolic shape. This is due to the fact that the temperature variation across the channel is minimized as the flow develops, resulting in a nearby uniform distribution of electrical conductivity σ. There is no heat generation due to the dissipative effect within the fluid because of the neglect of the viscous and Joulean terms ($Ek = 0$) in the energy equation; as the heat is conducted away from the fluid, the fluid temperature gradually approaches the wall temperature.

This phenomenon of M-shaped velocity profiles is not unfamiliar in MHD literature, as reported by Heywood [3], Thompson and Bopp [2], Oliver and Maxwell [28], and Branover [29]. It may be noted that the temperature-dependent electrical conductivity is not the only factor which can produce an overshoot velocity in the channel. Other factors resulting in a non-uniform Lorentz force distribution may also cause an M-shaped velocity distribution in the channel [2, 3, 28, 29].

Figure 11 represents a case where the viscosity, electrical conductivity, and thermal conductivity are all assumed to vary with respect to temperature with values of 0.5, 5.0, and 1.0 assigned to exponents α, β, and γ, respectively. As can be seen from Fig. 11, the velocity profile loses some of its M-shape while developing; however, unlike in Fig. 10, it retains its M-shape even when almost fully developed. This difference can be explained by noting that the viscous heating and Joulean heating are not neglected in the present case, and the heat generation in the fluid due to these dissipative effects prevents the total loss of temperature to the surroundings.

Although the thermal conductivity exponent was given a non-zero value in the last figure, the effect of the variation of γ on flow development has not been studied thus far. Of course, the variation of γ alone if σ and μ are held constant cannot affect the velocity distribution because it does not appear in the momentum equation. The variation of thermal conductivity with temperature plays an important role in the flow development, however, if the viscosity and/or electrical conductivity are also varied. An increase in the thermal conductivity of the fluid due to an increase in γ allows more of the heat generated by dissipation to be conducted away from the fluid. An interesting effect of the thermal conductivity variation on temperature can be seen in Fig. 12, where the viscosity and electrical conductivity are also allowed to vary. When exponent $\gamma = 0.0$, the increased amount of heat generation due to non-zero and positive values of α and β causes the temperature to rise sharply. With even relatively small values of γ, however, the temperature stabilizes quickly due to the increased ability of the fluid to conduct the heat away from it.

Figure 13 compares the bulk temperature variation in an MHD flow with constant properties and with cases when the exponents α, β and γ vary. When

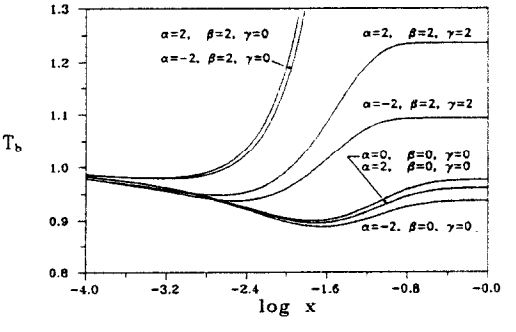

FIG. 13. Development of bulk temperature along the channel for $M = 20.0$, $R_E = -0.5$, $Pr = 0.75$, $Ek = 0.1$, and $\theta = 1.0$.

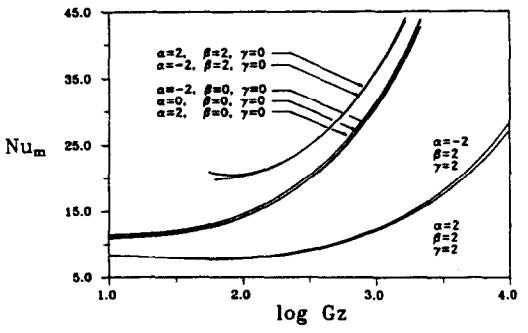

FIG. 14. Variation of average Nusselt number vs log of Graetz number for $M = 20.0$, $R_E = -0.5$, $Pr = 0.75$, $Ek = 0.1$, and $\theta = 1.0$.

$\alpha = 2.0$ or -2.0, the bulk temperature remains either slightly above or slightly below the constant property values. However, in the case when electrical conductivity also varies with temperature ($\beta = 2.0$), there is a sharp increase in bulk temperature for $\alpha = 2.0$ and -2.0, although for $\alpha = -2.0$ the bulk temperature is slightly lower than that for the case when $\alpha = 2.0$. Another situation observed in the figure is the effect of the variation of the thermal conductivity in combination with the variation of the other two properties. Figure 13 shows that while the temperature increased without bounds for the cases of $\alpha = 2.0$, $\beta = 2.0$, and $\gamma = 0.0$ and $\alpha = -2.0$, $\beta = 2.0$, and $\gamma = 0.0$, it stabilized to a fully developed state in both cases when γ was given a non-zero value of 2.0. This suggests that the variation of thermal conductivity with temperature must be taken into account if the results are to make physical sense.

Figure 14 is similar to Fig. 13, except that this figure shows the variation of average Nusselt numbers. As can be seen from Fig. 14, for any given values of β and γ, the variation of α from 2.0 to -2.0 does not cause much change in the Nusselt number values. However, for $\beta = 2.0$ there is an increase in the Nusselt number, and significantly there is a decrease in Nusselt number when γ, with a value of 2.0, is added to the problem.

SUMMARY AND CONCLUSIONS

The steady-state magnetohydrodynamic developing flow of an incompressible and viscous fluid between parallel electrically insulated plates maintained at constant and equal temperature has been investigated. The viscosity, electrical conductivity, and thermal conductivity of the fluid were assumed to be power-law functions of temperature. At the entrance of the channel, both velocity and temperature were assumed to be uniform, and the two were allowed to develop simultaneously. The governing equations, subject to the appropriate initial and boundary conditions, were solved by an efficient finite difference marching procedure which was found to be accurate and stable for a wide range of values of the parameters. A major portion of the results presented in this paper concentrated on the velocity, temperature, and heat transfer characteristics of the channel. However, the results for the variation of other parameters involved in the problem were also presented whenever their effects on velocity and temperature development were found to be significant. A more detailed set of results may be found in the first author's dissertation [21].

REFERENCES

1. R. J. Rosa, Design consideration for coal-fired MHD generator ducts, *5th Int. Conf. on MHD Electrical Power Generation*, Munich, Vol. 1, pp. 427–439 (1971).
2. W. J. Thompson and G. R. Bopp, The effects of variable properties on MHD flow in finite ducts, *J. Appl. Mech.* **37**, 954–958 (1970).
3. J. B. Heywood, An MHD channel flow with temperature dependent electrical conductivity, *AIAA J.* **3**, 1752–1754 (1965).
4. S. S. Filippov, Fluid flow with temperature dependent transport coefficients in a flat channel, *Magnitnaya Gidrodinamika* **6**, 81–85 (1970).
5. A. Setayeshpour, Magnetohydrodynamic Couette flow and heat transfer with variable viscosity and electrical conductivity, M.S. Thesis, Tennessee Technological University, Cookeville, Tennessee (1979).
6. A. M. Dhanak, Heat transfer in magnetohydrodynamic flow in an entrance section *J. Heat Transfer* **87**, 231–236 (1965).
7. R. C. LeCroy and A. H. Eraslan, The solution for temperature development in the entrance region of an MHD channel by the B. G. Galerkin method, *J. Heat Transfer* **91**, 212–220 (1969).
8. R. E. Schwirian, A new momentum-integral method for treating MHD and simple hydrodynamic entrance flows, AIAA Fluid and Plasma Dynamics Conf., Paper No. 69-724 (1969).
9. W. T. Snyder, Magnetohydrodynamic flow in the entrance region of a parallel-plate channel, *AIAA J.* **3**, 1833–1838 (1965).
10. C. L. Hwang, A finite difference analysis of magnetohydrodynamic flow with forced convection heat transfer in entrance region of a flat rectangular duct, Ph.D. Dissertation, Kansas State University, Manhattan, Kansas (1962).
11. J. L. Shohet, Velocity and temperature profiles for laminar magnetohydrodynamic flow in the entrance region of channel, Ph.D. Dissertation, Carnegie Institute of Technology, Pittsburgh, Pennsylvania (1961).
12. A. A. McKillop, J. C. Harper, H. J. Bader and A. Y. Korayem, Variable viscosity entrance-region flow of non-Newtonian liquids, *Int. J. Heat Mass Transfer* **13**, 901–904 (1970).
13. J. Lohrasbi, Magnetohydrodynamic heat transfer in two-phase flow with temperature-dependent properties, IEEE Int. Conf. on Plasma Sci., Crystal City, Virginia (1987).
14. M. L. Mittal, H. R. Nataraja and V. G. Naidu, Fluid flow and heat transfer in the duct of an MHD power generator, *Int. J. Heat Mass Transfer* **130**, 527–535 (1987).
15. A. Setayeshpour and V. Sahai, Heat transfer in variable-properties MHD entrance flow with a generalized temperature boundary condition, *Proc. 29th Heat Transfer and Fluid Mech. Inst.*, pp. 171–187 (1985).
16. S. T. Demetriades, C. D. Maxwell and D. A. Oliver, Progress in analytical modeling of MHD power generation—II, *Proc. 21st Symp. on Engng Aspects of Magnetohydrodynamics*, Argonne, Illinois (1983).

17. A. H. Hadid, Entry length effects in liquid metal fusion blankets, *Fusion Technol.* **10**(3), Part 2A, 854–859 (1986).
18. W. F. Hughes and F. J. Young, *The Electromagnetodynamics of Fluid*, Chap. 7. Wiley, New York (1966).
19. E. Doss, H. Geyer, R. K. Ahluwalia and K. Im, Two-dimensional performance analysis and design of MHD channels, *J. Fluids Engng* **103**, 307–314 (1981).
20. S. V. Patankar and D. B. Spalding, A finite difference procedure for solving the equations of the two-dimensional boundary layer, *Int. J. Heat Mass Transfer* **10**, 1389–1411 (1967).
21. A. Setayeshpour, Heat transfer in developing magnetohydrodynamic flow with variable transport properties, Ph.D. Dissertation, Tennessee Technological University, Cookeville, Tennessee (1984).
22. W. M. Flegal, A study of the velocity profile in the entrance region of a magnetohydrodynamic channel, Ph.D. Dissertation, Georgia Institute of Technology, Atlanta, Georgia (1970).
23. T. S. Chen and G. L. Chen, Magnetohydrodynamic channel flow on arbitrary inlet velocity profile, *Physics Fluids* **15**, 1531–1534 (1972).
24. H. Schlichting, Laminare kanaleinlau stromung, *Z. Angew. Math. Mech.* **14**, 368–373 (1934).
25. J. R. Bodoia and J. F. Osterle, Finite difference analysis of plane Poiseuille and Couette flow development, *Appl. Scient. Res.* **A10**, 265–276 (1961).
26. M. Roidt and R. D. Cess, An approximate analysis of laminar magnetohydrodynamic flow in the entrance region of a duct, *J. Appl. Mech.* **29**, 171–176 (1962).
27. R. Manohar, An exact analysis of laminar magnetohydrodynamic flow in the entrance region of a flat duct, *Z. Angew. Math. Mech.* **46**, 111–117 (1962).
28. D. A. Oliver and C. D. Maxwell, Interaction of magnetohydrodynamic plasma with boundaries, *AIAA 15th Aerospace Sci. Meeting*, Los Angeles (1977).
29. H. Branover, *Magnetohydrodynamic Flow in Ducts*. Wiley, New York (1978).

TRANSFERT THERMIQUE DANS UN ECOULEMENT MAGNETOHYDRODYNAMIQUE DE POISEUILLE AVEC PROPRIETES DE TRANSPORT VARIABLES

Résumé—On étudie l'effet de la variation avec la température des propriétés de transport sur le développement d'un écoulement magnétodynamique et sur le transfert thermique dans un canal à plans parallèles maintenus à des températures égales et uniformes. L'écoulement est supposé être permanent, laminaire et incompressible. Des résultats numériques représentatifs sont donnés pour montrer que la variation des propriétés, dans certaines conditions, peut avoir une influence sensible sur le développement des profils de vitesse et de température.

WÄRMEÜBERGANG IM ANLAUFGEBEIT EINER MAGNETOHYDRODYNAMISCHEN POISEUILLE-STRÖMUNG MIT VARIABLEN TRANSPORTEIGENSCHAFTEN

Zusammenfassung—Der Einfluß der temperaturabhängigen Eigenschaften auf eine sich entwickelnde magnetohydrodynamische Strömung und den Wärmeübergang in einem Kanal aus parallelen Platten von gleicher und konstanter Temperatur wird untersucht. Die Strömung wird dabei als stationär, laminar und inkompressibel angenommen. Typische numerische Ergebnisse werden dargestellt; dabei zeigt sich, daß die Veränderung der Eigenschaften unter bestimmten Bedingungen einen spürbaren Einfluß auf die Entwicklung von Geschwindigkeits- und Temperaturprofilen hat.

ТЕПЛОПЕРЕНОС ПРИ РАЗВИВАЮЩЕМСЯ МАГНИТОГИДРОДИНАМИЧЕСКОМ ТЕЧЕНИИ ПУАЗЕЙЛЯ С ИЗМЕНЯЮЩИМИСЯ СВОЙСТВАМИ ТЕПЛОПЕРЕНОСА

Аннотация—Исследуется влияние зависящих от температуры коэффициентов переноса на развитие магнитогидродинамического течения и теплоперенос в плоскопараллельном канале, на стенках которого поддерживаются постоянные и равные температуры. Предполагается, что течение является устойчивым, ламинарным и несжимаемым. Приводятся характерные численные результаты, которые показывают, что изменение характеристик переноса в определенных условиях может оказывать существенное влияние на развитие профилей скоростей и температур.